Journal of Civil Engineering and Urban Planning (2024)
Clausius Scientific Press, Canada

DOI: 10.23977/jceup.2024.060121
ISSN 2616-3969 Vol. 6 Num. 1

Research on Seismic Performance of Frame-Assembled Swing Wall

Qin Chen

School of Applied Science and Engineering, Fuzhou Institute of Technology, Fuzhou, 350506, China

Keywords: Swingwall; OpenSees; Assemble number; Assembly location

Abstract: Previous studies have shown that combining swing walls with frame structures to form a new type of frame swing wall can effectively improve the overall seismic performance of the structure. Based on this, this article proposes a new structural form of frame-assembled swing wall, in which the swing wall is vertically assembled by multiple wall pieces and connected to the foundation through unbonded prestressed steel bars to form a whole. A refined numerical analysis model for frame assembled swing wall was established based on the OpenSees numerical platform, and the accuracy of the model was verified through quasi-static tests of the frame structure and assembled swing wall structure. On this basis, combined with dynamic time history analysis, the seismic performance of the frame assembled swing wall was analyzed under different number of assembled wall pieces and different assembly positions. The results show that as the number of wall pieces increases, the stiffness of the frame assembled swing wall decreases to a certain extent, and the bending moment of the assembled wall decreases significantly. For example, when the number of wall pieces is 3, it decreases by 12.38%, and the seismic force under earthquake action is smaller. However, when the number of wall panels increases to 4, the interlayer displacement angle increases, leading to a deterioration in the seismic performance of the structure. Therefore, it is recommended to set the number of assembled wall pieces in the project to 2-3 sections. The analysis results also indicate that when the opening position is far from the weak layer of the frame and set at the lower part of the swinging wall, the interlayer displacement angle of the structural system is smaller, and the interlayer deformation is more uniform.

1. Introduction

Under earthquake action, frame structures often experience excessive lateral displacement of weak layers and uneven inter story deformation due to insufficient lateral stiffness. Therefore, adding swing walls to frame structures to form a frame swing wall system that can quickly assemble and reduce earthquake damage has become a research direction for many scholars.

Domestic and foreign scholars have conducted a series of studies on the frame-swinging wall system[1-5].Abroad, Ma et al. [6] conducted large-scale frame self resetting swing wall shaking table experimental research. The test results indicate that under earthquake action, the frame self resetting swing wall is basically undamaged and has excellent seismic performance. In China, Pei Xingzhu [7] designed a 10 story frame with 4 additional swing walls according to the specifications, and

conducted elastic-plastic analysis and nonlinear dynamic time history analysis comparison on frame shear walls of the same size. The results proved the superiority of the frame swing wall structure system. The above theoretical research and experimental results have proven the good seismic performance of swing structures.

However, when swinging walls are applied to multi-story buildings in practical engineering, the wall height is relatively high and construction is difficult. Therefore, the method of assembling multiple walls is generally adopted. Wiebe et al. [8] proposed a multi section slotted swing wall, which significantly reduces the internal force of the wall compared to traditional swing walls. Mohammad et al. [9] further studied and proposed a simplified analytical model for the above-mentioned swing wall. The study showed that the calculated results of the analytical model were in good agreement with the experimental results, and could be used for the design and analysis of such swing walls. The above research results provide a theoretical basis for the assembly of swing walls, but there has not been a systematic study on the number and location of swing wall assembly.

This article proposes the concept of "assembled swing wall" and forms a "frame assembled swing wall" system, and further studies the impact of different number of assembled wall pieces and different opening positions on the frame assembled swing wall structural system, providing reference basis for the future application of frame assembled swing wall.

2. Numerical modeling

In this study, the frame-assembled swing wall system is modeled by the Open System for Earthquake Engineering Simulation (OpenSees) software developed by the University of California, Berkeley. The modeling process consists of two main parts: the frame and the assembled swinging wall, as illustrated in Figure 1. Due to space limitations, this paper focuses on one method of connecting the beam between the frame and the assembled swinging wall, employing a two-node link unit simulation. The modeling techniques are described in detail in the subsequent sections..

2.1. Simulation of framework

The beams and columns of the frame are simulated using a distributed plastic hinge fiber element (ForceBeamColumn Element), and a fiber cross-section model is used. The fiber section includes concrete fibers and steel fibers, and the constitutive equations of Concrete02 material and Steel02 material are selected, respectively. The constitutive equations of concrete material consider the confinement effect of stirrups. The bottom of the frame is a fixed constraint, and the beam and column nodes are rigidly connected, as shown in Figure 1.

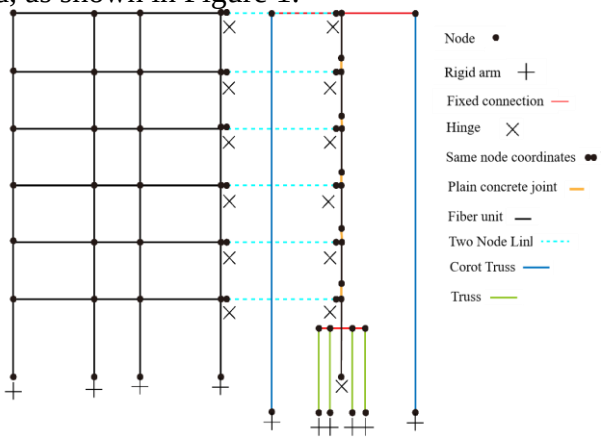

Figure 1: Frame - assembled swing wall simulation

2.2. Simulation of assembling a swinging wall

Figure 2 provides schematic diagrams of the models for assembling swing walls. From Figure 2, it can be seen that the modeling of the assembled swing wall mainly includes the simulation of wall sections, prestressed and energy consuming steel bars, wall section joints, and wall bottom connection methods. From Figure 2, it can be seen that the wall segments of the assembled swing wall are simulated using fiber elements, without considering their shear deformation. Both prestressed steel bars and energy consuming steel bars are unbonded, and are not established in the fiber section during modeling. The co rotating truss element CorotTruss element and Truss element are used for simulation, respectively. The unit length is the actual length of prestressed steel bars and energy consuming steel bars inside the wall. In order to simulate the position and anchoring situation of prestressed and energy consuming steel bars in the wall, the top of the prestressed and energy consuming steel bars is connected to the wall node through a rigid arm, and the bottom is a fixed boundary.

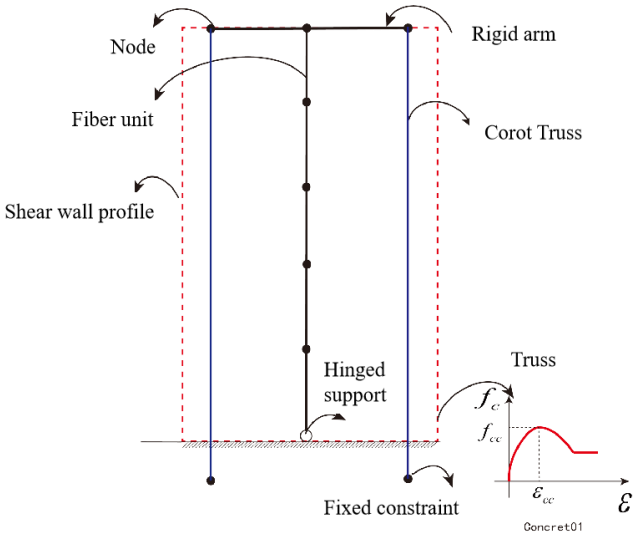

Figure 2: Simulation of assembling a swinging wall

The simulation of the slit position is the key and difficult point in the simulation of the assembled swing wall. Mortar is generally used for the opening of the wall section of the assembled swing wall, and the relationship between the selected element and the constitutive material needs to accurately simulate the characteristics of alternating tension and compression of the joint. Some scholars use zero length element combined with constitutive ent of uniaxial compression material to simulate the mechanical properties of joints. However, the constitutive model of ENT material only considers the elasticity of the material, and the simulation results can not accurately reflect the plastic damage behavior of concrete at the joint. However, the constitutive model of concrete01 concrete material accurately considers the compressive behavior of concrete without considering the tensile behavior, which conforms to the mechanical characteristics of joints. Therefore, according to the actual height of the joint, this paper uses fiber element simulation to simulate it, and gives the constitutive model of concrete 01.

3. Numerical model validation

In this section, the finite element software OpenSees is used to simulate the frame test of Tsinghua University [10] and the pseudo-static experiment conducted by foreign scholars Perez et al. [11] in ATLSS Laboratory of Lehigh University on the assembled shear wall with 5 reduced dimensions.

The results are compared with the test results. The feasibility and accuracy of the simulation method and boundary conditions for each part of OpenSees frame-assembled swinging wall system proposed in Section 2 are verified for further study.

3.1. Framework structure model validation

Tsinghua university designed a six story three span frame structure with reference to the relevant data of the Wenchuan earthquake. Due to the limitations of laboratory conditions, the prototype structure was reduced to a scale of 1:2 for quasi-static test. And publish all the test results (website: http://www.collapse-prevention.net) For relevant test data, see literature [10], and figure 3 is the layout of the test.

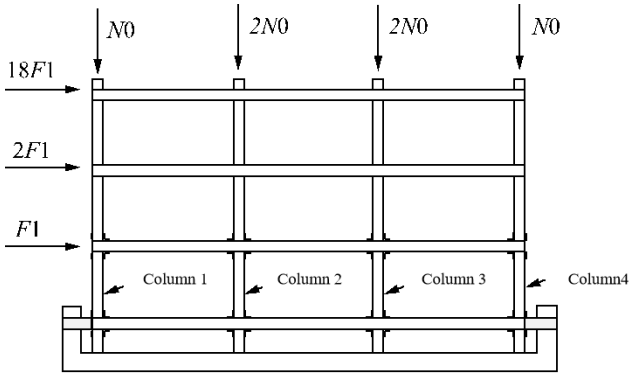

Figure 3: Frame structure test model

Figure 4 shows the comparison between the hysteretic curves and skeleton curves obtained by finite element calculation and the test results respectively. As can be seen from Figure 4, the finite element calculation results are in good agreement with the test results, which can better reflect the hysteresis and mechanical performance of the frame. However, there are some differences, mainly because when the test is loaded to the forward 150mm, the bearing capacity suddenly increases and enters the stage of decline, resulting in large differences in the simulation results. This is mainly because the role of the stirrup area of the column and beam and the ground beam is not considered in the model. However, the error of the yield point is less than 10% under positive and negative loading, and the error of the peak load is larger, but it is also less than 20%, which can accurately describe the hysteretic performance of the frame structure in general

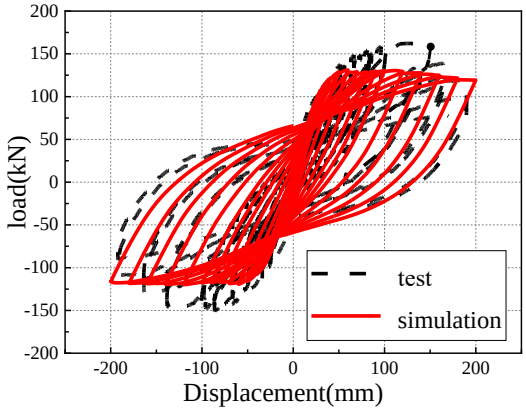

Figure 4: Hysteresis curve comparison.

3.2. Assembled swing wall model verification

In 2004, Perez et al. [11] designed and produced five scale assembled shear wall models and carried out quasi-static test research on them. The wall segments of the test members are connected only by post tensioned unbonded prestressed tendons. In this paper, TW2 specimens are selected for modeling and verification.

Figure 5 shows the comparison between the finite element calculation results and the test results of the hysteretic curve of the assembled swing wall. It can be seen from Figure 5 that the hysteretic characteristics of the assembled swing wall can be well simulated by using the fiber element and the concrete constitutive model of concrete01, and the stiffness and bearing capacity of the test piece calculated by the finite element method are relatively consistent with the test results.

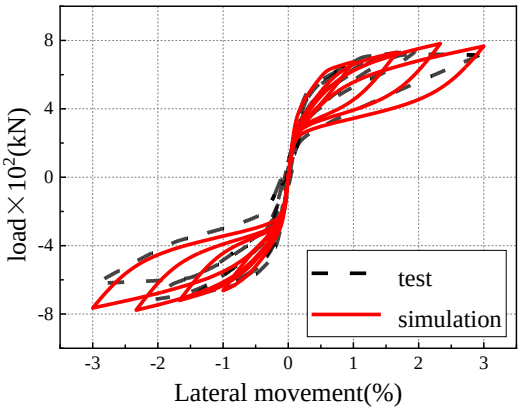

Figure 5: Hysteresis curve comparison.

4. Dynamic time history analysis of frame-assembled swinging wall

In this section, a six-layer frame is designed according to the code, and the stiffness of the swing wall is calculated according to the stiffness demand calculation formula of the swing wall obtained by Qu Zhe et al., and then the appropriate size and reinforcement of the swing wall are designed.

4.1. Frame model design

According to the seismic design code[12] and concrete structure design code[13] , a six-layer frame structure was designed, and its structural layout is shown in Figure 6. The site is designed with a basic wind pressure of 0.35kN /m2, and the ground roughness category is Class B. The top floor of the frame has a constant load of 1.5 kN/m2 and a live load of 2.0 kN/m2, while the rest of the floor has a constant load of 1.0 kN/m2 and a live load of 2.5 kN/m2. The section size of the frame beam is 250mm×500mm and the section size of the column is 550mm×550mm. PKPM is adopted for reinforcement design. The load distribution of the plane frame (load is converted into 1.0 dead load +0.5 live load) and the representative value of gravity load are shown in Figure 6. Among them, the strength grade of beam-and-column concrete is C30, the longitudinal reinforcement HRB400, and the stirrup HRB335. The 6-layer 3-span of axis 2 is taken as the object of subsequent numerical analysis.

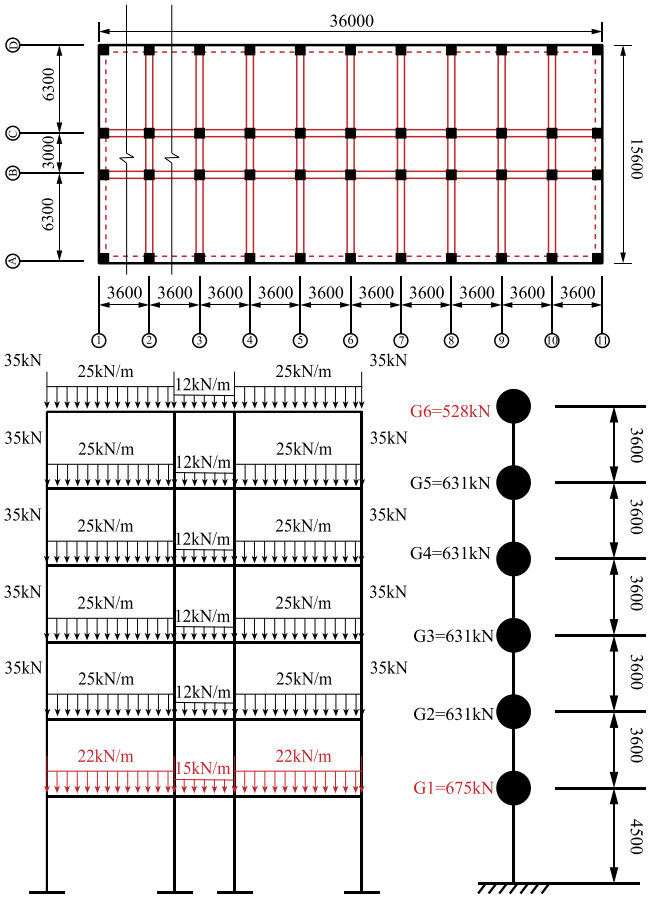

Figure 6: Frame structure design parameters

4.2. Model design for assembling swinging wall

The stiffness of swing wall has a significant impact on the seismic performance of frame swing wall system, so the stiffness ratio of frame and swing wall must be reasonably designed. A large number of scholars at home and abroad have carried out the research on the stiffness ratio of frame and swing wall. Among them, Qu Zhe[14] and others have given the calculation method of the required stiffness of swing wall with the goal of controlling the deformation mode of frame structure by swing wall.

In this paper, the size of the swing wall is designed by using the calculation formula verified by Qu Zhe and other relevant numerical models and theoretical analysis. The section size of the swing wall in this chapter is taken as 3000 mm ×250 mm, which meets the requirements. Figure 7 shows the reinforcement design of swing wall.

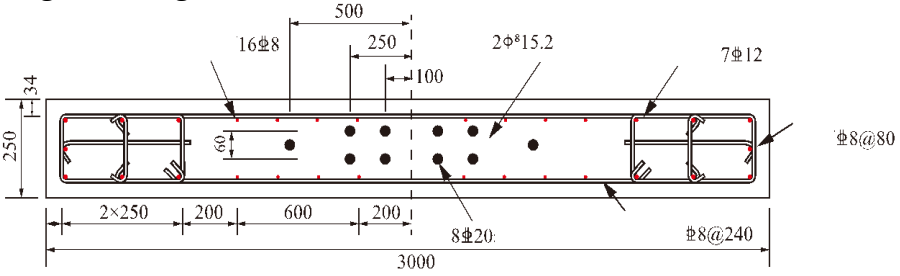

Figure 7: Assemble swinging wall reinforcement

4.3. Frame-assembly swinging wall model design

In this section, the frame and the assembled swing wall is connected by rigid rods, so that only horizontal force is transmitted between the frame and the swing wall.

In this paper, a frame assembled swing wall model with 1, 2, 3 and 4 pieces of assembled wall is designed. Considering the application problems in the actual project, and for the convenience of construction, when dividing the height of the assembled wall, the joint of the assembled wall shall be consistent with the beam height of the frame structure. The main design parameters are shown in Table 1. Where fptk is the standard value of prestressed reinforcement strength; Lu is the unbonded length of energy dissipation reinforcement; λ is the design value of bending moment contribution ratio.

Table 1: Main design parameters of specimens

Specimen number	Number of walls	Arrangement of prestressed reinforcement	Initial prestress fptk (N/mm)	Energy-consuming reinforcement configuration	Unbonded lengthLu/ mm	Vertical pressure/ kN
J-FSW	1	2As15.2	0.4	8 C 20	2500	730
J-FSW2	2	2As15.2	0.4	8 C 20	2500	730
J-FSW3	3	2As15.2	0.4	8 C 20	2500	730
J-FSW4	4	2As15.2	0.4	8 C 20	2500	730

Limited by space, this paper analyzes the assembled swing wall with different opening positions based on the model J-FSW2. Table 2 shows the slit position parameters of the finite element model for different slit positions.

Table 2: Assemble swing wall slot position

Specimen number	Slit position (from bottom)
J-FSW 2-1	3750mm
J-FSW 2-2	7500mm
J-FSW 2-3	11250mm
J-FSW 2-4	15000mm
J-FSW 2-5	18750mm

5. Dynamic time history analysis of frame-assembled swinging wall

5.1. Parameter analysis of different number of assembled wall pieces

5.1.1. Wall bending moment distribution

Figure 8 shows the comparison of wall bending moment of frame assembled swing wall with different number of wall pieces. Table 3 records the maximum bending moment and its average value of the wall.

It can be seen from Figure 8 that the internal force mode of each swing wall of the frame assembled swing wall model is the same, showing a "C" shape, the maximum bending moment appears in the middle, and the last bending moment is small. It can be seen intuitively from table 3 that with the increase of the number of wall pieces, the maximum bending moment of the frame assembled swing wall decreases significantly. Compared with J-FSW, J-FSW2, J-FSW3 and J-FSW4 decrease by 5.45%, 12.38% and 23.49% respectively. It shows that the increase of the wall reduces the stress of the wall, which improves the seismic performance of the structure.

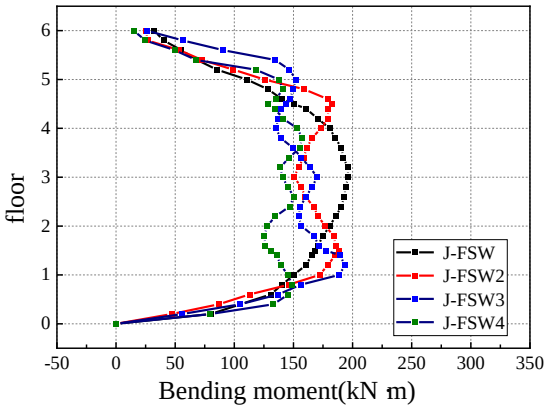

Figure 8: Wall bending moment of different wall pieces

Table 3: The maximum bending moment of wall with different number of wall pieces and its average value

model	Maximum bending moment(kN)	Mean value(kN)
J-FSW	196.265	196.265
J-FSW2	188.70	185.5691
	182.43	
J-FSW3	193.59	171.973
	170.13	
	152.19	
J-FSW4	148.81	149.396
	150.47	
	157.30	
	141.22	

5.1.2. Performance point parameter analysis

Table 4 shows the performance point parameters of different wall frame assembled swing walls under different seismic actions.

Table 4: Performance point parameters of different wall frame and assembled swinging wall under different seismic action

Structure type	Seismic intensity	Sa(g)	Sd(mm)
J-FSW	7(0.15g)	0.1647	140.4282
	8(0.3g)	0.2136	238.3894
	9(0.4g)	0.2236	301.2388
J-FSW2	7(0.15g)	0.1612	141.4713
	8(0.3g)	0.2014	250.1463
	9(0.4g)	0.2158	324.5126
J-FSW3	7(0.15g)	0.1567	145.3687
	8(0.3g)	0.1988	261.2847
	9(0.4g)	0.2057	336.2847
J-FSW4	7(0.15g)	0.1423	160.2546
	8(0.3g)	0.1751	290.2484
	9(0.4g)	0.1855	362.2548

It can be seen from the Sa value in Table 4 that with the increase of the number of wall pieces to 2, the Sa value of the frame assembled swing wall structure under the action of three seismic intensities decreases, which means that the seismic force on it decreases. When the number of wall pieces increases to 3, the effect on reducing the seismic force increases sharply, mainly because the more the number of wall pieces, the more obvious the reduction of the stiffness of the overall structure.

It can be seen from the Sd value in Table 4 that with the increase of the number of wall pieces to 2, the Sd value of the structure of the frame assembled swing wall increases under the action of three seismic intensities, and the lateral displacement of the structure increases. When the number of wall pieces increases to 3, the upward trend increases, mainly because the more the number of wall pieces, the more obvious the weakening of the lateral constraint of the whole structure.

5.1.3. Comparison of displacement angles between layers

Figure 9 shows the comparison curve of structural storey displacement angle of frame assembled swing wall corresponding to different wall number at 8 (0.3g) seismic performance points, in which the maximum storey displacement angle and storey displacement concentration factor DCF are summarized in Table 5.

It can be seen from Figure 9 that with the increase of the number of wall pieces, the maximum inter storey displacement angle of the frame assembled swing wall increases, but the inter storey displacement angle of the structure does not exceed the seismic code limit by 1/50. From table 5, when the number of wall pieces is 2 and 3, the inter storey displacement concentration factor DCF slightly increases, and when the number of wall pieces is 4, the value of DCF increases sharply. It can be seen that when the number of wall pieces exceeds 3, the deformation of the whole system will be uneven.

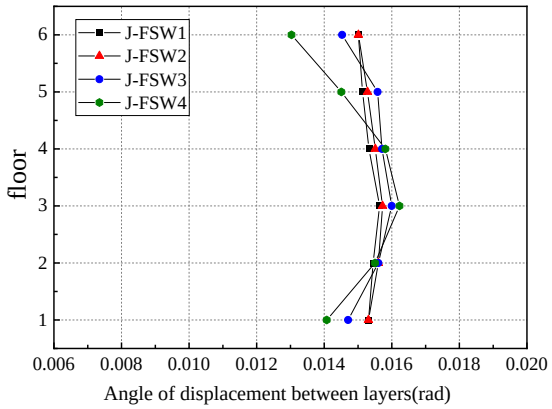

Figure 8: Comparison of displacement Angle curves between layers of different wall pieces

Table 5: The maximum interstory displacement Angle and interstory displacement concentration coefficient DCF of wall with different number of wall pieces

Structure type	Maximum interlayer displacement Angle	Concentration coefficient of interlayer displacement DCF
J-FSW1	0.01564	1.02
J-FSW2	0.01573	1.02
J-FSW3	0.0161	1.04
J-FSW4	0.01623	1.09

5.2. Parameter analysis of different assembly positions

5.2.1. Performance point parameter analysis

Table 6 shows the performance point parameters of different wall panel frames - assembled swing walls under different seismic actions. It can be seen from table 6that when the slit position is below the middle, the Sa value of the structure under the three seismic intensities basically does not change, and when the slit position is above the middle, the Sa value decreases to a certain extent, but the impact is small.

It can be seen from the table that when the slit position is below the middle, the Sd value of the structure under the action of three seismic intensities is basically the same. When the slit position is above the middle, the Sd value increases to a certain extent, which means that the lateral displacement of the structure increases.

Table 6: Performance point parameters of frame-assembled swinging wall at different assembly positions under seismic action

Structure type	Seismic intensity	Sa(g)	Sd(mm)
J-FSW 2-1	7(0.15g)	0.1658	137.4215
	8(0.3g)	0.2055	247.2874
	9(0.4g)	0.2198	327.2158
J-FSW 2-2	7(0.15g)	0.1637	138.2587
	8(0.3g)	0.2067	248.3658
	9(0.4g)	0.2143	323.2678
J-FSW 2-3	7(0.15g)	0.1612	138.4713
	8(0.3g)	0.2014	250.1463
	9(0.4g)	0.2158	324.5126
J-FSW 2-4	7(0.15g)	0.1552	145.2874
	8(0.3g)	0.1957	253.3254
	9(0.4g)	0.1989	328.2574
J-FSW 2-5	7(0.15g)	0.1517	152.2587
	8(0.3g)	0.1865	258.9854
	9(0.4g)	0.1939	335.1478

5.2.2. Comparison of displacement angles between layers

Figure 10 shows the comparison curve of the inter story displacement angle of the frame structure corresponding to different wall numbers at 8 (0.3g) seismic performance points, in which the maximum inter story displacement angle and the inter story displacement concentration factor DCF are summarized in Table 7.

It can be seen from Figure 10 and table 7 that with the increase of the number of walls, the maximum inter story displacement angle increases, but the structural inter story displacement angle does not exceed the seismic code limit by 1/50. At the same time, when the number of walls is 2 and 3, the inter story displacement concentration factor DCF increases slightly, and when the number of walls is 4, the value of DCF increases sharply. It can be seen that the deformation of the whole system will be uneven when the number of walls exceeds 3.

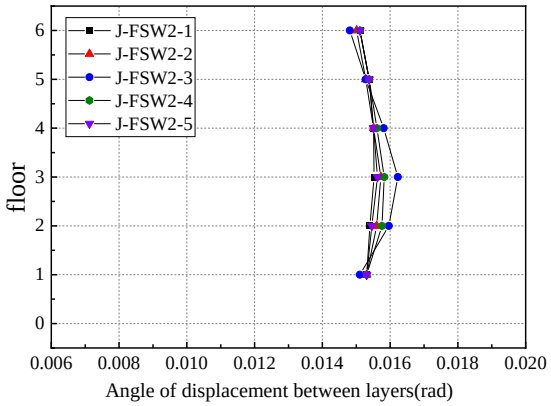

Figure 10: Displacement Angle between two walls at different opening positions

Table 7: Maximum interlayer displacement Angle and interlayer displacement concentration coefficient at different assembly positions

Structure type	Maximum interlayer displacement Angle	Concentration coefficient of interlayer displacement DCF
J-FSW2-1	0.0154	1.11
J-FSW2-2	0.01578	1.12
J-FSW2-3	0.01623	1.22
J-FSW2-4	0.01583	1.17
J-FSW2-5	0.01561	1.13

6. Conclusion

Based on the OpenSees numerical platform, a refined numerical analysis model of the frame assembled swing wall system is established. The accuracy of the model is verified by the quasi-static test results of the frame structure, and the assembled swing wall structure. On this basis, the dynamic time history analysis of the frame assembled swing wall system with different wall pieces and different slit positions is carried out. The conclusions are as follows:

With the increase of the number of wall pieces, the stiffness of the frame assembled swing wall decreases to a certain extent, and the bending moment of the wall decreases significantly, thus reducing the damage of the wall. However, the corresponding maximum storey displacement angle is larger, and the effect on the deformation control of the whole frame system is worse. Therefore, it is suggested that the number of wall pieces should be 2-3;

When the assembly position of the frame assembled swing wall is close to the weak layer of the frame structure, the greater the interlayer displacement angle, the worse the effect of the swing wall on the deformation control of the whole frame system. Therefore, it is suggested that the joint position is close to the middle of the frame structure, which can better improve the seismic performance of the structure.

References

[1] Clough R W, Huckelbridge A A. Preliminary experimental study of seismic uplift of a steel frame[M]. Earthquake Engineering Research Center, College of Engineering, University of California, 1977.

[2] Ajrab J J, Pekcan G, Mander J B. Rocking Wall–Frame Structures with Supplemental Tendon Systems[J]. journal of structural engineering asce, 2004,130(6):895-903.

[3] Xu Jiaqi, LüXilin. Energy based seismic response of frame-rocking-wall structure and frame-shear-wall structure.[J], Building Structure, 2013,43(S2):418-422.
[4] Qu Zhe. Study on Seismic Damage Mechanism Control and Design of Rocking Wall-Frame Structures[D].Tsinghua University,2010.
[5] Qu Zhe, Ye Lieping. Seismic damage mechanism control of rocking wall-frame system[J].Earthquake Engineering and Engineering Vibration, 2011,31(04):40-50.
[6] Deierlein G, Ma X, Hajjar J, et al. Large-scale shaking table test of steel braced frame with controlled rocking and energy dissipating fuses[C]// 9th US National and 10th Canadian conference on earthquake engineering. 2010.
[7] Pei Xingzhu, WANG Pei. Research on seismic Performance of Concrete frame-swing wall System [J]. Seismic Engineering and Reinforcement,2013,35(02):19-28.
[8] Wiebe L, Christopoulos C. Mitigation of higher mode effects in base-rocking systems by using multiple rocking sections[J]. Journal of Earthquake Engineering, 2009,13(S1):83-108.
[9] Khanmohammadi M, Heydari S. Seismic behavior improvement of reinforced concrete shear wall buildings using multiple rocking systems[J]. engineering structures, 2015,100:577-589.
[10] LU Xinzheng, Ye Liping, Pan Peng, Zhao Zuozhou, JI Xiaodong, Qian Jiaru. Test Research on pseudo-static Collapse of Reinforced Concrete Frame Structure and Numerical Simulation Competition I: Frame test [J]. Journal of Architectural Structures, 2012,42(11):19-22+26.
[11] Perez F J, Sause R, Pessiki S. Analytical and Experimental Lateral Load Behavior of Unbonded Posttensioned Precast Concrete Walls[J]. journal of structural engineering asce, 2007,133(11):1531-1540.
[12] Code for seismic design of buildings(GB50011-2010)[S]. Bei Jing:China Architecture & Building Press,2010
[13] Code for design of concrete structures(GB50010-2010)[S].Bei Jing:China Architecture & Building Press,2010
[14] QU Zhe. Research on seismic damage mechanism control and design Method of swing Wall-Frame Structure [D]. Tsinghua University, 2010.